Comprehensive Review and Analysis of Two-element Resonant Compensation Topologies for Wireless Inductive Power Transfer Systems

K. N. Mude[1*] *and K. Aditya*[2]
(1. Systec R&D, Porto, Portugal;
2. University Ontario Institute of Technology, OShawa, Canada)

Abstract: Wireless power transfer (WPT) is gaining much attention for battery charging of electric vehicles (EVs). Resonant WPT systems play a crucial role in achieving efficient power transfer from source to load. An overview of two-element resonant compensation techniques and their characteristics under various operating conditions are presented. Also the converter and control strategies used for different topologies are reviewed. The behavior of the performance factors are evaluated against the operating conditions and compared for the different topologies.

Keywords: Resonant wireless power transfer, compensation topologies, power converters, battery charging

1 Introduction

Wireless power transfer systems (WPTSs) transfer power from supply (grid) to load without any galvanic connection [1-5]. Wireless charging of electric vehicle (EV) batteries offers a number of advantages compared to the wired counterpart such as safety, water-resistance, durability, possibility of in-motion charging, better industrial design, and aesthetics (lack of clutter). WPTSs are hence expected to play a major role in future EV charging equipment [6-7].

The general scheme of WPTS is shown in Fig. 1. It consists mainly of two sections: transmitting (or primary) and receiving (or secondary), each of them includes a coil that is coupled to the other one with a large air-gap in between. Both the WPTS sections are equipped with power conversion circuitry. On the transmitting section, the grid feeds the relevant coil through a capacitor-output diode rectifier and an in-cascade inverter operating at high frequency. Grid, rectifier, and inverter constitute the power supply for the transmitting coil and are equivalent to a power supply formed by a voltage generator and an internal resistance. Only the fundamental component of the voltage delivered by the generator is of interest for the energy transfer so that the generator can be considered sinusoidal. On the receiving section, the voltage induced across the receiving coil charges the battery through another capacitor-output diode rectifier and an in-cascade chopper, which adapts its output current/ voltage to the battery charging requirements. Rectifier, chopper, and battery constitute the load of the receiving coil and are equivalent to a resistance [8-15].

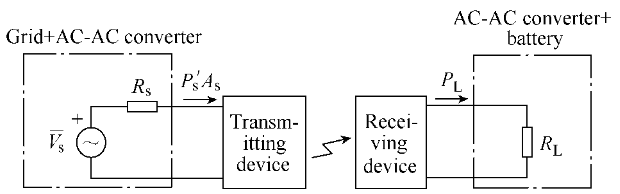

Fig. 1 Wireless power transfer (WPT) system

The major concern of a WPTS is an air gap between the coupling coils, which leads to large leakage inductance and small mutual inductance. This results in a large primary current requirement in order to transfer given amount of power [16]. This high current increases loss in the system, which leads to poor efficiency. A method to overcome this problem is to compensate the reactive elements by using capacitors, so that only resistive elements remain in the system, which reduces the losses caused by circulating current, thereby efficiency will increase [17-25]. Primary-side compensation decreases VA rating of the source side converter thereby ensuring power transfer at unity power factor, while secondary compensation enhances power transfer capability of the system [16].

Arrangement of capacitor in a WPT plays a crucial role in behavior of the system. Capacitor(s) can be arranged in different ways resulting in single resonant compensation [26-28], and multi resonant

* Corresponding Author, Email: kishore.308@gmail.com
Digital Object Identifier: 10.23919/CJEE.2019.000008

compensation [29-56], (using two and three elements) respectively, with series or parallel arrangement or both. In two-element resonant topology (TERT) four fundamental topologies of resonant WPTSs can be arranged: series-series (SS), series-parallel (SP), parallel-series (PS) and parallel-parallel (PP), depending on how the capacitors are inserted in the two sections of the WPTSs [8-10]. Under the category of three element resonant topologies (THERT), SSP (LLC) [44, 58], and SPP (LCC) [47], and double sided LCC [55], topologies are investigated.

Power flow in WPT system can be controlled from the primary side or the secondary side or the combination of both [70]. Choice of control depends upon the architecture and application of the WPT system. For an inductive power transfer (IPT) system with multiple receiver coils coupled to a single transmitter coil, primary current and frequency are maintained constant, and power flow regulation is maintained on the secondary side by the combination of rectifier and DC-DC converter for each receiver coil [70]. Power flow regulation can be obtained by one of many methods such as shorting control or variable frequency control on the secondary side. This type of architecture and control is very common in material handling system and monorail or automatic guided rail system where supply and track are required to provide power to a number of independent loads [71-72]. For charging application where there is only one receiving coil coupled to the transmitting coil, it is better to use primary side control. This eliminates the additional DC-DC converter stage but has a simple rectifier and filter [73]. This architecture eliminates additional losses incurred in DC-DC conversion stage which in turn leads to considerable efficiency gain even at light load condition as compared to secondary side control. This has added benefit in biomedical implants because it makes the system compact and light enough to be inserted inside the skin [74]. A combination of both primary side and secondary side regulation is being used in bidirectional WPT system to send power from vehicle to grid (V2G) [75-79]. However, it requires extra components and control which need to be justified, given there is less time available to consider power flow back to the grid. Moreover, frequent charging and discharging of EV battery reduces its life. Hence there is a tradeoff between actual energy recovered and money invested in maintenance and replacement of car batteries.

This paper carries out a thorough review of the characteristics of the resonant WPTS pertaining to dynamic WPT charging. Section 2 introduces a basic overview of single resonant and multi resonant topologies. Section 3 analyses the characteristics under different operating conditions such as varying load, varying coupling coefficient, frequency mismatch, and component tolerances respectively. Section 4 reviews the converters and control of resonant topologies. Section 5 compares the different aspects of the resonant topologies, and Section 6 concludes the paper.

2 Resonant WPT system

2.1 Inductive WPTS

The electric circuitry of an inductive WPTS is drawn in Fig. 2, where L_T and L_R are the self-inductances of the transmitting (primary) and the receiving (secondary) coils, M is their mutual inductance, and R_S and R_L are the source and load resistances. A parameter that is crucial in assessing the performance of the inductive WPTSs is the coupling co-efficient of the two coils, given by [3]

$$k \triangleq \frac{M}{\sqrt{L_T L_R}} \tag{1}$$

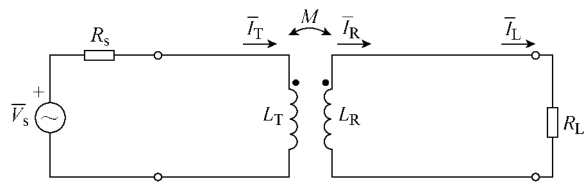

Fig. 2 Inductive WPT circuitry

Voltage equations of the transmitter and receiver sections are

$$\begin{cases} \overline{V}_s = \dot{Z}_T \overline{I}_T + j\omega M I_R \\ 0 = j\omega M I_T + \dot{Z}_R \overline{I}_R \end{cases} \tag{2}$$

Where $\overline{Z}_T$ and $\overline{Z}_R$ are the impedances of the transmitter and receiver sections, given by

$$\begin{aligned} \dot{Z}_T &= R_S + j\omega L_T \\ \dot{Z}_R &= R_L + j\omega L_R \end{aligned} \tag{3}$$

and ω is the angular frequency of $\overline{V}_S$ from formula (2), the currents flowing in the transmitter and receiver sections are given as

$$\begin{cases} \bar{I}_{\mathrm{T}} = \dfrac{\bar{V}_{\mathrm{S}}}{\dot{Z}_{\mathrm{T}} + \dfrac{\omega^2 M^2}{\dot{Z}_{\mathrm{R}}}} \\ \bar{I}_{\mathrm{R}} = \dfrac{\bar{V}_{\mathrm{S}} \dfrac{\mathrm{j}\omega M}{\dot{Z}_{\mathrm{T}}}}{\dot{Z}_{\mathrm{R}} + \dfrac{\omega^2 M^2}{\dot{Z}_{\mathrm{T}}}} \end{cases} \tag{4}$$

From formula (4), it is observed that the transmitting current ($\bar{I}_{\mathrm{T}}$) is co-related with Z_{T} and $(\omega M)^2/Z_{\mathrm{R}}$, where $(\omega M)^2/Z_{\mathrm{R}}$ is referred to as the receiver-to-transmitter reflected impedance, labeled as Z_{rt}. Similarly $(\omega M)^2/Z_{\mathrm{T}}$ is the transmitter-to-receiver reflected impedance, labeled as Z_{tr}. The load power and efficiency of inductive WPT can be given as [18]

$$P_{\mathrm{L}} = \frac{P_{\mathrm{L}} V_{\mathrm{S}}^2 \omega^2 M^2}{\left\| \dot{Z}_{\mathrm{T}} \dot{Z}_{\mathrm{R}} + \omega^2 M^2 \right\|^2} \tag{5}$$

$$\eta_{\mathrm{i}} = \frac{R_{\mathrm{L}} \omega^2 M^2}{\left| \dot{Z}_{\mathrm{R}} \right|^2 Re\left| \dot{Z}_{\mathrm{T}} \right| + \omega^2 M^2 Re\left| \dot{Z}_{\mathrm{R}} \right|} \tag{5a}$$

Usually efficiency is expressed as a function of the parameter k and the quality factors of transmitter (Q_{T}) and receiver (Q_{R}) of the coils, defined as

$$\begin{cases} Q_{\mathrm{T}} \triangleq \dfrac{\omega L_{\mathrm{T}}}{R_{\mathrm{S}}} \\ Q_{\mathrm{R}} \triangleq \dfrac{\omega L_{\mathrm{R}}}{R_{\mathrm{L}}} \end{cases} \tag{6}$$

Substitution of formulas (3) and (6) into formula (5) leads to [8]

$$\eta_{\mathrm{i}} = \frac{k^2 Q_{\mathrm{T}} Q_{\mathrm{R}}}{1 + Q_{\mathrm{R}}^2 + k^2 Q_{\mathrm{T}} Q_{\mathrm{R}}} \tag{7}$$

2.2 Necessity of compensation

In an inductive WPT, without secondary resonant capacitors, power transfer to the load cannot be sufficient unless the input voltage is large. The reason is that the impedance of the receiver coil is large and therefore is responsible for significantly reducing the current in the load resistance. One solution is to increase the input voltage so that the power transferred to the load is sufficient, but this is not optimal because it requires higher current in the primary coil, which in turn generates greater energy losses, thus reducing efficiency. Therefore, these resistances are required to be as small as possible. At the same time, the self-inductance of the coils has to be maximized, since it represents their ability to generate a magnetic flux intensity for a given current. Generally, high inductance goes with high resistance, so there is a trade-off with an optimal solution for every application which has to be investigated. The goal is then to use coils with the highest possible quality factor.

The previous point leads to necessary addition of resonance capacitors (RCs) to the transmitter and receiver sides. By decreasing or even cancelling the large reactance of a coil, the RCs allow to reduce the current amplitudes and therefore to improve the efficiency of WPT system, and the optimum is reached at the resonance frequency. RCs involve an alternating exchange of energy between the capacitor and the inductance of the coil, and the amount of energy required to maintain the oscillation is minimal. RCs are used in WPT applications in order to minimize VA rating of the power converter and maximize the power transfer capability， make constant current or constant voltage，increase the efficiency and the power transfer capability of the system they are used in，and obtain zero phase angle (ZPA) to avoid bifurcation analysis. These capacitors store and supply reactive power to and from the secondary and primary, reducing the amount of reactive power drawn from the supply.

2.3 Level of compensation

Level of compensation is quantified by means of quality factor of the transmitter (Q_{T}) and receiver (Q_{R}). Quality factors Q_{T} and Q_{R} are important parameters to decide the VA ratings of transmitter, receiver and power transfer capability. The choice of Q_{R} is an important consideration in deciding the amount of power transferred, the larger Q_{R} envies the higher power transfer capability of the WPT system. The ratio of Q_{T} to Q_{R}, may be grouped into one of three categories namely $Q_{\mathrm{T}}>Q_{\mathrm{R}}$, $Q_{\mathrm{T}}=Q_{\mathrm{R}}$, and $Q_{\mathrm{T}}<Q_{\mathrm{R}}$. From a stability point of view, it is preferable that $Q_{\mathrm{T}}>Q_{\mathrm{R}}$, but this does not always result in the most cost-effective design [21].

2.4 Bifurcation phenomenon

In Ref. [29], authors explained the bifurcation and frequency splitting phenomenon of the WPT system. A bifurcation phenomenon occurs when a system has more than one zero phase angle frequency. It has been shown in Refs. [31-39] that the bifurcation phenomenon highly depends on the quality factors of the coils. So to avoid the bifurcation phenomenon in the WPT system, the quality factor of transmitter should always be greater than that of the receiver coil and thus the system will operate on a single zero angle frequency. The condition for quality factor, to achieve ZPA is tabulated in Tab. 1.

Tab. 1 Quality factor dependency on bifurcation phenomenon [39]

Topology	Condition for quality factor
SS	$Q_R < \sqrt{\dfrac{1}{2\left(1-\sqrt{1-k^2}\right)}}$
SP and PS	$Q_R < \dfrac{1}{k}\sqrt{1-k^2}$
PP	$Q_R < \dfrac{1}{k}$

2.5 Performance factors (PF)

Prior literature proposes various performance factors and parameters such as efficiency (η), power supply sizing factor (PSSF), receiving coil sizing factor (RCSF) [18], power factor (PF) [19], per unit magnitude of load current (PUMLC), voltage ratio (M_v), current ratio (M_i) [27]. The quantities in formulas (8) and (9) are P_L, P_S, A_S, A_R, I_L, and $V_S/\omega M$, which are the active power absorbed by the load, the active and apparent powers delivered by the power supply, the apparent power of the receiving coil, the load resistance current, and the base value of current, respectively. V_R, V_S, I_R, I_S are receiver voltage, source voltage, receiver current, and source current respectively.

$$\eta = \frac{P_L}{P_S}, \alpha = \frac{A_S}{P_L}, \beta = \frac{A_R}{P_L}, I_{L,(ptt)} = \frac{I_L}{V_S/\omega M} \tag{8}$$

$$PF = \frac{P_L}{A_S}, M_v = \frac{V_R}{V_S}, M_i = \frac{I_R}{I_S} \tag{9}$$

2.6 Compensation alternatives

Schematic diagram of receiver and transmitter compensation is shown in Fig. 3. Impedances of the resonant tank for series (Z_{ser}) and parallel $\left(Z_{par}\right)$ configurations are given as

$$Z_{ser} = Z_L + Z_C \tag{10}$$

$$Z_{par} = \frac{Z_L Z_C}{Z_L + Z_C} \tag{11}$$

where Z_L and Z_C are inductive and capacitive impedances respectively.

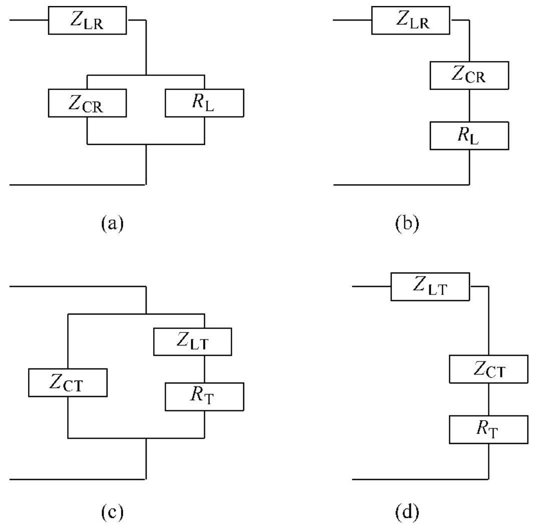

Fig. 3 Transmitting and receiving section compensation

Substituting values of Z_L and Z_C in formulas (10) and (11), then series and parallel impedances become

$$Z_{ser} = j\frac{(\omega_o^2 L_T C_T - 1)}{\omega C_T} \tag{12}$$

$$Z_{par} = \frac{\omega C_T}{j(\omega_o^2 L_T C_T - 1)} \tag{13}$$

At resonance, impedance of series RLC circuit becomes minimum, while impedance of parallel RLC circuit becomes maximum. Under such conditions the receiver impedance and reflected impedance from secondary to primary is given as

$$Z_{R,ser} = R_L, Z_{R,par} = \frac{\omega_o^2 L_R^2}{R_L - j\omega_o L_R} \tag{14}$$

and the reflected series and parallel resistances are given as

$$Z_{Rtr,ser} = \frac{\omega_o^2 M^2}{R_L} Z_{Rtr,par} = \frac{M^2 R_L}{L_R^2} - j\frac{\omega_o^2 M^2}{L_R} \tag{15}$$

Total impedance of the primary as seen by voltage source is given as

$$Z_{Tot} = \frac{Z_R L_T^2}{M^2} - j\omega_o L_T \tag{16}$$

2.7 Resonant topologies (RTs)

The RTs can be classified depending on reactive structures into single-resonant and multi-resonant types. The single-element resonant structures associate a capacitor to each coil whereas multi-resonant topologies employ multiple reactive components in the transmitter and/or the receiver side. The two compensation capacitances C_T and C_R for the main topologies give two degrees of freedom in the system. In addition to their simplicity, there exists a wider study on the single-resonant structures so that some design guidelines have already been identified [25-29] and the detailed analysis explained further in following sections.

(1) Single element resonant topologies (SERT).The different types of single resonant topologies is shown in Fig. 4 and it can be grouped as transmitter and receiver compensation. Theoretically, the power transfer capability of receiving coil will be effective only when system operates at resonant frequency which is given by

$$\omega = \frac{1}{\sqrt{L_R C_R}} \tag{17}$$

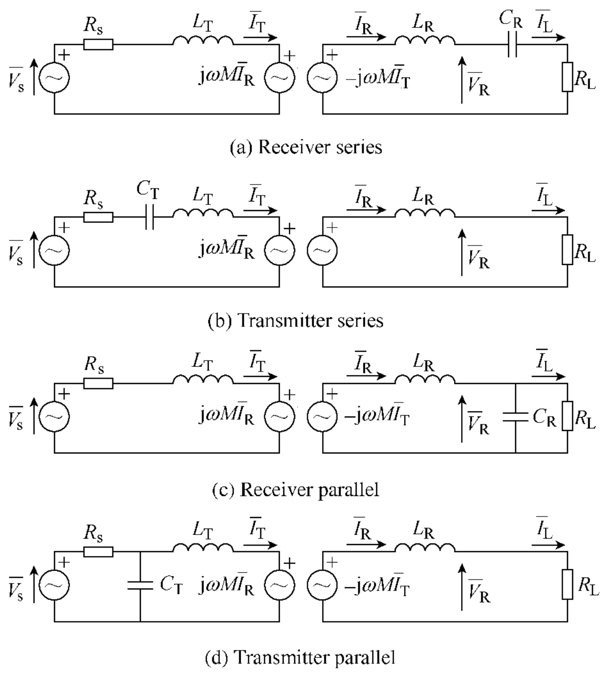

Fig. 4 SERT

The simplest SERT compensation circuit that contains only a capacitor in series with the transmitter has been studied by authors [21-22], and in Refs. [24-25], the single resonant topologies analyzed based on voltage gain, current gain and power factor for four different cases shown in Fig. 4, and concluded that except for the transmitter series structure, in which power factor can reach a high level (near to unity) for any Q_R, and the other three compensation topologies have very low pf for normal values of Q_R. Power factor of transmitter series topology can reach unity only when the load is very heavy, and for secondary parallel topology, only when the load is very light which reveals that the series compensation is not able to satisfy all the requirements.

The simple impedance matching techniques using capacitor in the receiving side, are elaborated in Ref. [35], and in Refs. [28-29], authors proposed an additional transformer behind the capacitor that would reduce the total transmitter inductance "seen" by the capacitor. Both of these methods are not suitable because of dependency of load and transmitter current, and VA ratings of the capacitor which is unacceptable for high power applications. And also the conclusion drawn from Ref. [8], claims that series insertion of a capacitor modifies only the imaginary part of the impedances. On the other hand, the efficiency according to formula (5a) is a function of both the imaginary and real parts of Z_R, and only of the real part of Z_T. Therefore, the insertion of a capacitor in series to the transmitting coil does not affect the WPTS efficiency. Instead, the WPTS efficiency is affected and enhanced by inserting a capacitor in series to the receiving coil and by choosing for the capacitor a value that makes it resonating with L_R at the angular frequency ω.

From the above discussions, it is clear that SERTs are not able to preserve a constant primary current for different load or coupling conditions. Therefore, the analysis that follows below focused on multi resonant topologies.

(2) Multi resonant topologies (MRTs). Multi component topologies use two or more capacitors and numerous ways of the connecting resonant tanks considered in Refs. [27-39] as shown in Fig. 5 and Fig. 6. All of them have been investigated in Refs. [40-42]. MRTs can be further divided into two distinct categories namely: two element resonant topologies (TERT) and three element resonant topologies (THERT). TERT can be classified as series-series (SS), series-parallel (SP), parallel-series (PS), and parallel-parallel (PP) are widely adopted [17-18]. The SS and SP topologies were more commonly used in literature as voltage-fed resonant converter power supplies, whose resonant networks require series-tuning at the input port, are

more readily accessible. For SP compensation, the circuit is easily mistuned since the primary compensated capacitance relates to the coupling. In comparison, the compensation capacitance can be a constant value for fully-compensated SS method regardless of the coupling and load variation. However, it has poor output voltage regulation capability [15]. The PS and PP topologies, requires additional inductor in series which increases the complexity of the system. The traditional TERT can't solve the most of the issues such as capacitance tolerances and voltage regulation. This can be improved by using THERT such as LLC and LCC resonant topology [49-55]. In Ref. [59], excellent

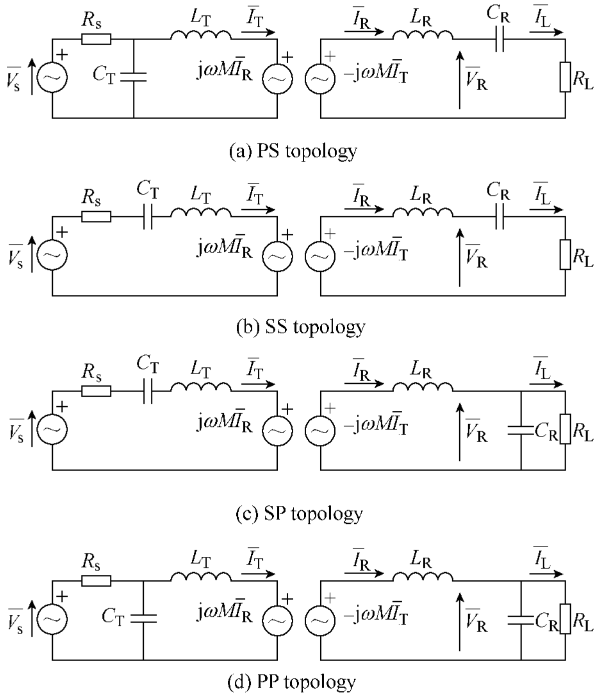

Fig. 5 TERT resonant topologies

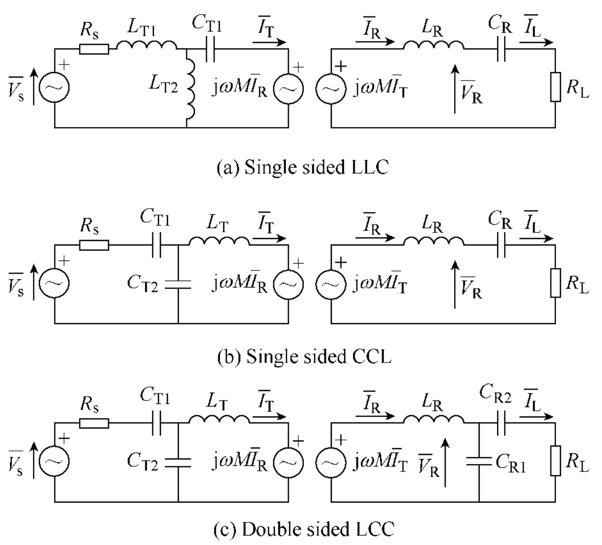

Fig. 6 THERT

explanation is provided why the LCL topology is so successful. Authors state that it effectively integrates the load matching feature of the parallel scheme with the characteristic of the series compensation to include all parasitic inductances of the resonant circuit and power switches. Additionally, its overall structure allows inherent protection against a short circuit condition anywhere on the transmitter [63]. The feature of the load independent track current is a unique characteristic of this topology.

For LCC circuit an inductor of LLC is replaced by a capacitor as shown in Fig. 6b. By utilizing LCC compensation network, a zero current switching (ZCS) condition could be achieved by adjusting capacitor parameters [57]. Also, when this compensation is applied in the secondary side, the reactive power at the secondary side could be compensated to form a unit power factor pickup [61]. To further improve the stability of the system, the double sided LCC topology shown in Fig. 6c proposed in Ref. [47], in which topology and tuning method ensure that the resonant frequency is independent of coupling coefficient and load conditions, and the ZVS condition for the Switch is realized. However, the inductances of the additional inductors and capacitor increases the complexity of the circuit as well as the control aspects of the circuit.

Each topology has its own merit and demerit and it is not possible to present a detailed analysis of each in the same paper, therefore focus of the paper will be on TERT topology in proceeding sections. A detailed analysis of TERT to identify its operating conditions in terms of load variation, coupling coefficient, frequency variations and component tolerances thereby answering the questions regarding the operating loading conditions and frequency optimization and power transfer efficiency has been presented in detail in next sections.

3 Analysis of the resonant topologies

The compensation capacitance (CC) values are function of the parameters of the coil. For the TERT, the secondary compensation capacitance has to be selected as the first step. The primary one has to be computed as the second step. The order of these steps is not mandatory but is mere convenience since the value of the secondary compensation capacitance is independent of the primary one but the primary compensation capacitance depends on the secondary one [39]. The modelling and design guidelines of the selection of compensation capacitors is mostly based on the coil self, mutual inductances and resonant frequency which are shown in the appendix. From formulas (5) and (7), it can be observed that, the PFs of the resonant topologies are functions of load resistance (R_L), coupling coefficient (k), frequency (f) and component tolerances (ct)

$$PF = \text{func}\left(R_L, k, f, ct\right) \tag{18}$$

The analysis performed for the one of the PF is efficiency, in that case the first derivative of the efficiency with function of control variables as follows

$$\left\{ \frac{\partial}{\partial\left(R_L, k, f, ct\right)}\left(\eta_i\right) = 0, i = 0,1,2,\cdots,n \right. \tag{19}$$

3.1 Load

In the applications of multiple battery charging systems where load continuously changes, the topology selection problem becomes difficult as we can choose a load in favour of either topologies and hence one left with the question of which topology to use under any loading conditions. The load characteristics of the WPT system are very important to model the coil when the load resistance R_L is variable. Formula (19) emerges as mostly PFs depends on function of load, for example, the efficiency is increases up to one when frequency increases and moreover, by observing the charging profile in Ref. [17], the R_L increases abruptly at about 100 times of the constant voltage mode. So it is interesting to evaluate characteristics under varying load condition [20-21].

Refs. [17-18, 21] describe the condition that depends on the load. In applications where the load is variable, such as in EV battery charging, meeting of formula (17) entails that the supply frequency must be continuously tuned to maintain the resonance condition in the receiving section, and if the resonance condition is maintained in the receiving section, this can be not done in the transmitting section where the resonance frequency is fixed. The main concern about the resonant topologies is change of receiving quality factors. It is worth to note that the quality factors of the receiving and transmitting sections in the resonance conditions can be expressed as

$$Q = \frac{1}{\omega CR} \tag{20}$$

Tab. 2 Values of transmitter capacitance and quality factors of transmitter and receiver [91]

Topology	Transmitter capacitance	Transmitter quality factor (Q_T)	Receiver quality factor (Q_R)
SS	$\frac{L_R C_R}{L_P}$	$\frac{L_R R_S}{\omega M^2}$	$\frac{\omega L_R}{R_L}$
SP	$\frac{L_R{}^2 C_T}{L_T L_R - M^2}$	$\frac{\omega L_T L_R^2}{M^2 R_L}$	$\frac{R_L}{\omega L_S}$
PS	$\frac{L_T}{\left(\frac{M^2}{L_R C_R R_L}\right)^2 + \frac{L_T{}^2}{L_R C_R}}$	$\frac{L_T R_L}{\omega M^2}$	$\frac{\omega L_R}{R_L}$
PP	$\frac{\left(L_T L_R - M^2\right) L_R{}^2 C_R}{M^4 R_L^2 C_R + \left(L_T L_R - M^2\right)^2}$	$\frac{\omega L_T L_R^2}{M^2 R_L}$	$\frac{R_L}{\omega L_S}$

From Section 2, it is observed that the equivalent impedance Z_T is inversely proportional to the load resistance R_L. Thus, the system is short-circuited, if it is driven by a constant voltage because the current becomes zero. Removing the load or the secondary part of the coils leads to a huge primary current (theoretically infinity).

In Ref. [20], the impact of efficiency, PSSF, RCSF and PULMCs are well explained with respect to load variation for the four types of topologies and comparison with traditional one is made, shown in Fig. 7 and Fig. 8, which claimed that the SS topology is a better option for the case of varying load. Taken to evaluate the characteristics of a WPTS, analytical expressions of them have been worked out for the resonant WPTSs with all four topologies, and as an point of reference for the inductive WPTSs. As an example characteristics of efficiency, PSSF is shown in Fig. 7 and Fig. 8, and it has appeared that the resonant WPTSs with the SS topology are the best overall choice because they feature many merits such

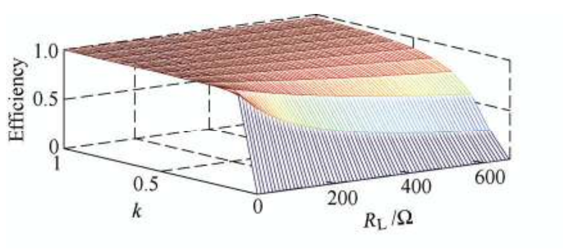

Fig. 7 Efficiency of different topologies and of inductive WPTSs vs. R_L and k [18]

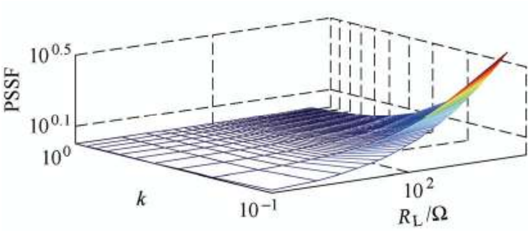

Fig. 8 PSSF of different topologies and of inductive WPTSs vs. R_L and k [18]

as higher efficiency, lower power supply sizing factor, higher p.u. magnitude of the load resistance current, and lower sensitivity to the quality factor of the receiving section. The only shortcoming is the higher receiving coil sizing factor that increases with the quality factor of the receiving section.

Most of the literature focused on the efficiency oriented compensation but in Ref. [37], authors introduced a novel compensation methodology called "control-oriented compensation" with the aim is to cancel the reactance of the coil and to get the value of the capacitances independently of the load value. Although the efficiency is not maximal compared to efficiency-oriented compensation, a high value is still obtained. And authors also claimed that the behavior of the WPT system can be either a voltage or current source for all topologies in the control-oriented compensation which is unlike in the efficiency-oriented compensation where a current source for SS topology and a voltage source for PS topology. However, the load voltage V_L is function of the load current I_L for the SP and PP topology. One can note that for the two controls at imposed currents, an additional closed-loop control must be used. Tab. 3, compares the efficiencies of the above two oriented methodologies.

Tab.3 Efficiency-oriented v.s. control-oriented [37]

Topology	By applying constant voltage	
	Efficiency-oriented	Control-oriented
SS	$I_L = \frac{V_S}{\omega M}$	$I_L = \frac{V_S}{\omega M}$
SP	$I_L = \frac{M}{L_T}\sqrt{\left(V_S^2 - M^2\omega^2 I_L^2\right)}$	$V_L = \frac{M}{L_T}V_S$
PS	$V_L = \frac{V_S L_R}{M}$	$V_L = \frac{V_S L_R}{M}$
PP	$V_L = \frac{M}{L_T}\sqrt{\left(M^2 V_S^2 - \left(M^2 - L_T L_R\right)\omega^2 L_T^2\right)}$	$I_L = \frac{M}{\left(L_T L_R - M^2\right)\omega}V_S$
Topology	By applying constant current	
	Efficiency-oriented	Control-oriented
SS	$V_S = \omega M I_L$	$V_S = \omega M I_L$
SP	$I_L = \frac{L_T}{M}I_S$	$I_L = \frac{L_T}{M}I_S$
PS	$I_L = \frac{M}{L_R}I_T$	$L_T = \frac{M}{L_R}I_T I_L = \frac{M}{L_R}I_T I_L = \frac{M}{L_R}I_T$
PP	$V_L = \frac{\left(L_T L_R - M^2\right)\omega I_T I_L}{\left(L_R M\right)^2 I_L^2 - I_T^2 M^4}$	$V_L = \frac{\left(L_T L_R - M^2\right)I_T}{M}$
Topology	Coil driven with constant primary coil current	
	Efficiency-oriented	Control-oriented
SS	$V_L = \omega M I_S$	$V_L = \omega M I_S$
SP	$V_L = \omega M I_S$	$V_L = \omega M I_S - \frac{\omega M^2}{L_T}I_L$
PS	$I_L = \frac{M}{L_R}I_T$	$I_L = \frac{M}{L_R}I_T$
PP	$I_L = \frac{M}{L_R}I_T$	$I_L = \frac{M}{L_R}I_T$

In Refs. [32-34], authors proposed the equivalent circuits and mathematical models based on the circuit theory. The formulas of transfer efficiency and the system efficiency of these four topologies are deduced.

With certain parameters, the transfer efficiency of the four topologies is proved to be the same. However, the system efficiency of the primary parallel connection is higher than that of the primary series connection. Making resonant the receiver stage endowed the WPTs with the lowest variations of efficiency and power supply sizing factor due to variations of their reactive parameters.

3.2 Frequency

Increasing the power by increasing the frequency is something of an illusion and may not bring about the benefits expected. This has been explained below:

Since the frequency of interest in WPT system usually lies from 20 kHz to 200 kHz [89] and the litz wire is the common choice for winding purpose. However, litz wire is selected based on operating frequency range. For example, for 50-100 kHz of frequency range, one will select a litz wire made of 40AWG strand [86]. Therefore, operating the system made of 40AWG wire with 100 kHz or more will give no advantage of litz wire effect and therefore copper losses will increase with increasing frequency. Operating below 50 kHz is also not recommended since then litz wire will be underutilized as they are expensive and therefore using wire made of 40 AWG for less than 50 kHz is not a good design choice. IPT system with and without core has been presented in Ref. [90]. Choice of core type also depends on operating range of frequency. For example, 3F3 ferrite magnetics from Ferro Cube Company can operate in the frequency range from 200 kHz to 500 kHz, while 3C90 ferrite magnetics can only work below 200 kHz [91]. Again these are selected at design level only, and therefore operating frequency should not be deviated from permitted operating range of selected core material.

Varying the frequency within the operating range can affect the system either adversely or irrefutably and cannot be predicted beforehand without having any experimental results. Increasing the frequency (within permitted range of use) at same voltage lowers the flux density in air-gap and the core material. This permit the use of smaller volume of core material. However, it also increases the core losses and therefore without experimental results it is hard to find an optimum frequency which gives the PF in WPT system. Even for air cored coils inductances of circuit such as mutual inductance and self-inductance of coil pair varies with frequency variation. Besides this heat generation in switching circuit increases with increasing losses.

Based on above discussion it is safe to say that for a designed WPT system optimum frequency can only be decided through experimental analyses or FEA analysis. And therefore finding an optimum frequency for high PF will be not presented in this paper.

3.3 With varying coupling coefficient

When the receiver coil is positioned above the transmitter coil, the coupling coefficient (k) between the coils is proportional to the ratio of the overlapped area of the coils to the area of the transmitter coil and inversely proportional to the third power of the distance between the coils. This leads to a coupling coefficient lower than the expected one.

Refs. [13, 27, 37] report performance of efficiency under varying k, for different values of Q_R. The graph claims that PS and PP topologies maintains higher values throughout k and the SS topology behavior is the same as PS and PP for the higher values of k. SP and inductive coupling follow the same behavior of SS but efficiency is less.

3.4 Components tolerances

When the transmitter inductor or capacitance is varied, the reactive impedance on the transmitter side no longer cancels each other out. For the resonant WPTS, the components inductances, L_T, L_R and capacitors C_T, C_R are subject to variation with the different operating conditions which depends on the frequency of operation, and changes in the load and environmental conditions which affect the resonant condition in WPT system.

In Ref. [69], authors investigated the effect of variation of self-inductances and capacitances for the SP and PS topologies. In which they claimed that variations in the C_T, when is in the series with the transmitter coil strongly impact on the efficiency and the load voltage. For the SP topology, the value of efficiency is reduce by 30%, for the variation of 10 % of C_T and PS topology efficiency is unaffected. Instead it shows the opposite behavior for both SP and PS topologies, for the load variation when variation of the C_R. On the other hand, modifications of the L_T provoke a decrement of the system efficiency. Diminishing of 10% of this inductance makes the efficiency be reduced up to a 30% in the SP topology and a 20% in the PS topology. The variations of the inductance which is in parallel with the capacitance is associated to an incremented load voltage. However, for the SP topology, this occurs when the secondary inductance is increased. Under these circumstances, the efficiency is drastically degraded for the PS topology.

In Ref. [91], authors explained that the topologies with a series compensated transmitter side are very sensitive to a decreased distance between the two coils. The change in self-inductances due to the opposite core increases the reactive currents of the system and decreases the power factor. Reactive currents lead to additional losses in the system. On the other hand, increasing the distance between the two coils does not affect the power factor, and the efficiency remains high. Increasing the distance between the two coils by 10 cm only slightly decreases the efficiency.

4 Converter and control for resonant topologies

4.1 Converter

Converter and control depends upon the type of compensation topology and application of WPT system respectively. Although most WPT systems are based on two stage AC-DC-AC conversion, there have been attempts to achieve direct AC-AC conversion from grid [80]. IGBT based push-pull converter [81] were famous during early stage of WPT development but due to recent advances in the MOSFET technology for medium voltage (600-1 200 V) and an increase in the switching frequency have made full bridge MOSFET-based topologies as widely accepted power converter topology [82-83]. For primary series compensation topology voltage-source converter is preferred and for primary parallel current-source converter is preferred. However, since voltage-source converter has been proven to be more efficient, having higher reliability and faster dynamic response. Therefore, voltage-source converter is converted into current-source converter by either operating in current controlled mode or connecting a series inductance in series with the DC link forming current fed topology or connecting series inductance in primary side forming LLC topology. Since full bridge converter offers more control possibility it is generally preferred over half bridge topology. At frequency range in excess of 10 kHz-10 MHz power amplifier is generally used. Today, there are several classes of power amplifiers available such as class A, class AB, class C, class D and class E. Among these, class D and class E amplifiers are the mostly used at high frequency because of their ability to provide a great efficiency at such frequency [84]. Fig. 9 shows all primary side converter topology used for WPT system transferred high frequency power is rarely directly delivered to the load, and a power conditioner is necessary to transform it into DC power or controllable AC voltage [85].

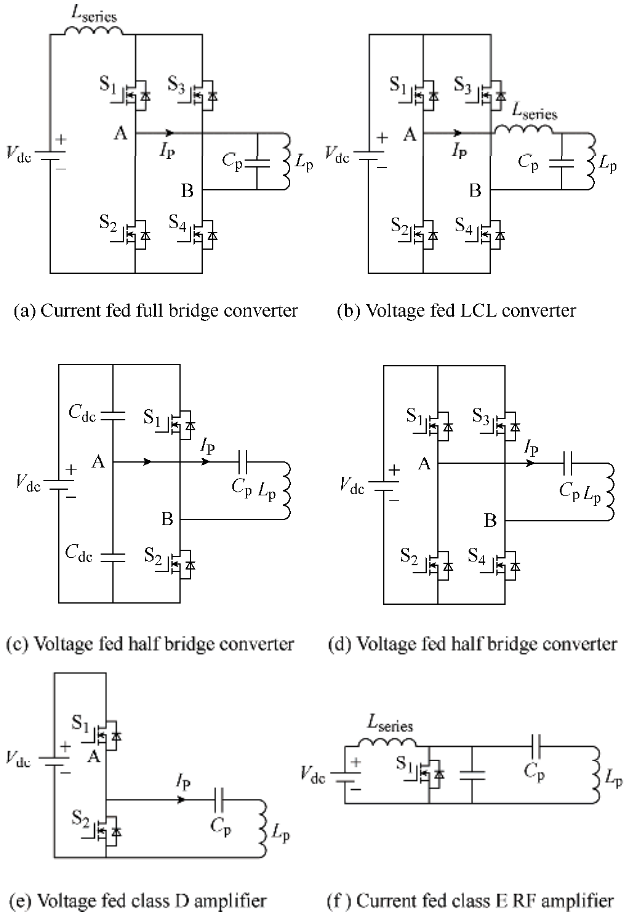

Fig. 9 Primary side converter

A power conditioner is used to maintain the specified voltage or current to the load in the face of changes in coupling between coils and load variation.

The type of power conditioner used is a function of the compensation circuit structure. It almost always contains a rectifier, and DC-DC converter with a smoothing output filter. When miniaturization is an important goal for the receiver design, as in the case of an implantable medical WPT receiver, the power conditioner might be simplified, consisting of only the rectifier [86]. Apart from these the primary and the secondary sides are equipped with all necessary sensors and control circuits to generate the firing signals for switches and to control transferred power. Additionally, communication modules might be installed, which add a further level of intelligence and controllability to the system. Fig. 10 shows the two most common type converters used in WPT system.

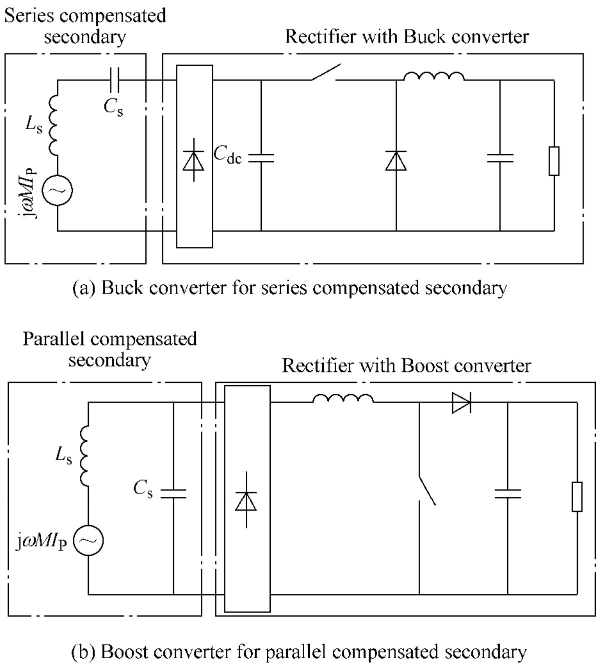

Fig. 10 Buck converter for series compensated secondary and Boost converter for parallel compensated secondary

4.2 Control

Power flow regulation in WPT system can be achieved by primary side control or secondary side control or combination of both [87]. However, application of two controller in both primary and secondary sides will not only increase the cost but also render the system less reliable [88]. Therefore, either primary side control or secondary side control will be less costly and reliable solution for a WPT system. Both primary side control and secondary side control can be variable frequency or fixed frequency control. With primary control DC-DC converter after rectifier can be eliminated but it does require a wireless communication link between the primary and secondary side to enable safe power regulation. Primary side regulation can be achieved by varying the DC link voltage, controlling the switching frequency or controlling the phase shift between the two legs of the inverter (fixed frequency control).

Varying the DC link voltage will require an additional power electronic device, for example a DC-DC converter, which induce more losses into the system and makes system costlier. Variable frequency control works on the principle of maintaining zero phase angle frequency in primary side with varying load and mutual inductance. However, relation between power transfer in WPT system and frequency has found to be linear therefore deviating much from resonant frequency or perfect tuning condition will affect the peak power transfer capability of the system [89]. Moreover, it may also result in a loss of frequency stability and controllability because of the onset of bifurcation with increasing load, where more than one primary ZPA frequency exists. Therefore, variable frequency control should be avoided wherever possible such as in the case of series-series topology where compensation is unaffected by load or mutual inductance variation. Therefore, for variable frequency control narrow band frequency range control should be used. There are mainly three narrow frequency-range control techniques used for control of resonant converters, namely asymmetric duty cycle control (ADC), asymmetrical voltage cancellation control (AVC) and phase shift control (PS) [19]. These three control strategies can be used in both fixed frequency mode and variable frequency mode. Fig. 11 shows the switching scheme and waveform of all three control strategies for full bridge converter.

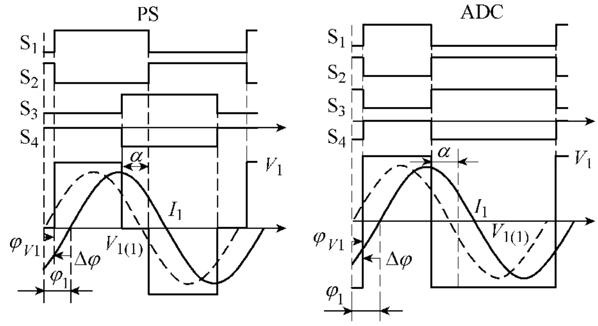

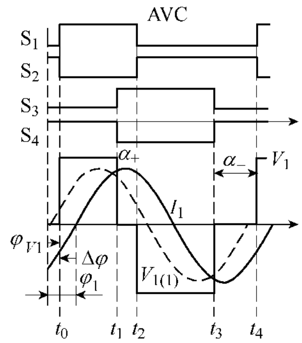

Fig. 11 Narrow frequency band control strategies

However, primary side control strategies maintain the power flow regulation by varying the primary input voltage or primary input current which will affect all the secondary pickup and some of the pickup may be unable to deliver the necessary power. Therefore, primary side control is more suited with WPT system having only one pick-up such as for charging applications. For multiple pick-up system secondary side control is preferred and an additional DC-DC converter is employed to maintain the desired voltage and current required for the load. This allows each pick-up to be controlled separately or even decoupled completely from the primary. However, it increases the cost, switching losses and compromises the reliability of the system.

Besides having unidirectional power flow there have been attempts to maintain bidirectional power flow especially in the case of electric vehicle charging system using WPT. However how much power can be generated by this means and how much extra cost would be incurred in replacing the batteries need to be taken into consideration before adopting such control scheme. Since bidirectional power flow requires batteries to be charge and discharge more frequently than unidirectional power system and this compromises the life of the battery. Besides this solution might work for only stationary charging application since in the case of dynamic charging there is little time available to consider power flow back to the mains and it may not bring the desired benefits as expected.

5 Comparison of resonant topologies

The two-element topologies are compared for different PFs at different operating conditions such as variation of load, coupling-coefficient and component tolerances etc. Result obtained are tabled in Tab. 4.

Tab.4 Comparison of TERT

Parameters	Topologies			
	SS	SP	PS	PP
Output	Current source	Voltage source	Voltage source	Current source
In sensitive to changes in	Receiver capacitance (C_R)	Receiver capacitance (C_R)	Transmitter capacitance (C_T)	Transmitter capacitance (C_T)
Efficiency	Very high	Lower	Lower	High
PSSF	Very high	Lower	Lower	Lower
RCSF	Low	High	Low	Low
Normalized current	High	High	Low	Low
Equivalent impedance	Minimum	Minimum	Maximum	Maximum
Tolerance of efficiency on variable frequency	Lower	Higher	Lower	Higher
Output power	High	High	Low	Low
Control alternatives	Output current	Output voltage	Output voltage	Output currnet
Sensitivity to distance	Very much sensitive	Very much sensitive	Less sensitive	Less sensitive
Pf @distance	Unaffected	Unaffected	Increases	Increases
Dependent on Load	No	Yes	Yes	Yes

The power factor of the SS compensation topology is unaffected by the increased distance. With an increased distance the output levels increase. This means that the topologies with a series compensated primary side are well suited for transferring large amounts of power over large distances. The topologies with a parallel compensated primary side are less sensitive to a decreased distance between the two coils than the topologies with a series compensated primary side. The efficiency is increased when the two coils are moved closer to each other. The power factor is reduced when the distance between the two coils is increased however, and so is the efficiency. With a decreased distance the output levels increase. This means that the topologies with a parallel compensated primary side are well suited for transferring large amount of power over small distances. The comparison of various topologies is provided in Tab. 4.

In the Fig. 12a, the efficiency is observed against load variation, which claims that in light load condition, series compensation is preferable to the parallel compensation, when the load is smaller impedance than the impedance of compensation capacitors, where as in parallel compensation, the parallel impedance is dominated by the load, so the resonant condition is weakened. In the Fig. 12b, the efficiency is observed against coupling coefficient, where for all topologies, for the lower value of *k*, efficiency is low and it increases with increased value of *k*. The complete PFs dependency of the TERT are tabulated in Tab.4.

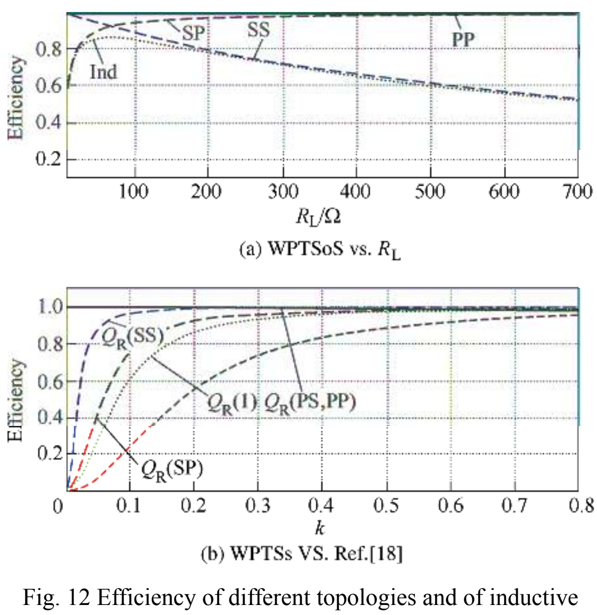

Fig. 12 Efficiency of different topologies and of inductive

Fig. 13 shows the measurement results for the efficiency against load resistance which are well agree well with the values of simulated and analytical results[5].

6 Conclusions

This paper presented a thorough review of the

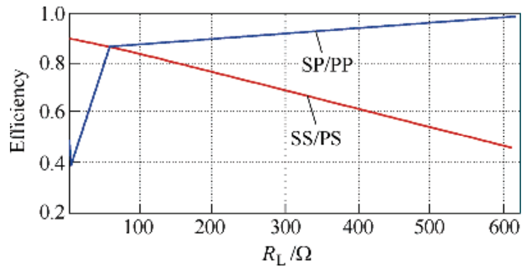

Fig. 13. Measurement of different topologies vs. R_L

WPT system. The paper discussed the single element resonant topologies as well as multi element resonant topologies. It is shown that mutual inductance, and quality factor of transmitter and receiver are the three most important parameters of the WPT system which determine its characteristics. While mutual inductance directly influences the efficiency of WPT system, quality factor on the other hand determines the VA rating and stability of the system. Selection of material such as litz wire and core material has also been discussed briefly. In addition, the paper discussed different types of converter and control methodologies which have been in use for WPT based EV battery charger.

References

[1] L Jiangui, Y Qingxin, C Haiyan, et al. Study and application of contactless electrical energy transmission system. *Proc. of IEEE Vehicle Power and Propulsion Conference*, 2008: 1-4.

[2] D J Thrimawithana, U K Madawala. A contactless bi-directional power interface for plug-in hybrid vehicles. *Proc. of IEEE Vehicle Power and Propulsion Conference*, 2009: 396-401.

[3] M P Kazmierkowski, A J Moradewicz. Unplugged but connected: review of contactless energy transfer systems. *IEEE Industrial Electronics Magazine*, 2012, 6(4): 47-55.

[4] J M Miller. Wireless power charging fundamentals and challenges. *Proc. SAE Hybrid Veh. Technol. Symp*, 1-17.

[5] G Buja, M Bertoluzzo, K N Mude. Design and experimentation of WPT charger for electric city-car. *IEEE Transactions on Industrial Electronics*, 2015, 62(12): 7436-7447.

[6] S Lukic, Z Pantic. Cutting the cord: Static and dynamic inductive wireless charging of electric vehicles. *IEEE Electrification Magzine*, 2013, 1(1): 57-64.

[7] S Y R Hui, W C Ho. A new generation of universal contactless battery charging platform for portable consumer electronic equipment. *IEEE Transactions on*

Power Electronics, 2005, 20(3): 620-627.

[8] M Bertoluzzo, R Jha, G Buja. Series-series resonant IPT system analysis under frequency mismatch. *Proc. of IEEE Industrial Electronics International Conference (IECON)*, 2015: 439-444.

[9] G A Covic, J T Boys. Inductive power transfer. *Proc. of IEEE*, 2013, 101(6): 1276-1289.

[10] A P Sample, D A Meyer, J R Smith. Analysis, experimental results, range adaptation of magnetically coupled resonators for wireless power transfer. *IEEE Transactions on Industrial Electronics*, 2011, 58(2): 544-554.

[11] C S Wang, O H Stielau, G A Covic. Design considerations for a contactless electric vehicle battery charger. *IEEE Transactions on Industrial Electronics*, 2005, 52(5): 1308-1314.

[12] O H Stielau, G A Covic. Design of loosely coupled inductive power transfer systems. *Proc. of IEEE Conference on Power System Technology*, 2000, 1: 85-90.

[13] J Li, Q Yang, H Chen, et al. Study and application of contact-less electrical energy transmission system. *Proc. of IEEE Vehicle Power and Propulsion Conf.*, 2008: 1-4.

[14] G A Covic, J T Boys. Modern trends in inductive power transfer for transportation applications. *IEEE Transactions on Emerging Sel. Topics in Power Electronics*, 2013, 1(1): 28-41.

[15] B Choi, J Nho, H Cha, et al. Design and implementation of low-profile contactless battery charger using planar printed circuit board windings as energy transfer device. *IEEE Transactions on Industrial Electronics,* 2004, 51(1): 140-147.

[16] E Abel, S Third. Contactless power transfer-an exercise in topology. *IEEE Transactions on Magnetics*, 1984, 20(5): 1813-1815.

[17] K N Mude, M Bertoluzzo, G Buja. Design of contactless battery charger for electric vehicle. *Proc. of IEEE AFRICON*, 2013: 1099-1104.

[18] K N Mude. Wireless power transfer for an electric vehicle. Padua: University of Padua, Italy, 2015.

[19] L Chen, S Liu, Y C Zhou, et al. An optimizable circuit structure for high-efficiency wireless power transfer. *IEEE Transactions on Industrial Electronics*, 2013, 60(1): 339-349.

[20] M Bertoluzzo, K N Mude，G Buja. Characteristic evaluation of wireless battery chargers for electric vehicles. *Proc. of IEEE Electromotion*, 2013: 1-5.

[21] J T Boys, G A Covic, A W Green. Stability and control of inductively coupled power transfer systems. *Proc. of IEEE EPA*, 2000, 147(1): 37-43.

[22] A P Hu, J T Boys, G A Covic. ZVS frequency analysis of a current-fed resonant converter. *Proc. of 7th IEEE Power Electronics Congress*, 2000: 217-221.

[23] W Chwei-Sen, G A Covic, O H Stielau. Power transfer capability and bifurcation phenomena of loosely coupled inductive power transfer systems. *IEEE Transactions on Industrial Electronics*, 2004, 51(1): 148-157.

[24] A Khaligh, S Dusmez. Comprehensive topological analysis of conductive and inductive charging solutions for plug-in electric vehicles. *IEEE Transactions on. Vehicular Technology*, 2012, 61(8): 3475-3489.

[25] R Fernandes, J Matos, N Carvalho. Constructive combination of resonant magnetic coupling and resonant electrical coupling. *Proc. of IEEE WPTC*, 2015: 1-3.

[26] D Fernandes, R Matos, J N Borges, et al. Resonant electrical coupling: circuit model and first experimental results. *IEEE Transactions on Microwave Theory and Techniques*, 2015, 63(9): 2983-2990.

[27] Z Pantic, S Bhattacharya, S Lukic. Optimal resonant tank design considerations for primary track compensation in inductive power transfer systems. *Proc. of IEEE Energy Conversion Congress and Exposition (ECCE)*, 2010: 1602-1609.

[28] L Grajales, F Lee. Control system design and small-signal analysis of a phase-shift-controlled series-resonant inverter for induction heating. *Proc. of IEEE PES*, 1995, 1: 450-456.

[29] Z Yiming, Z Zhengming, C Kainan. Frequency decrease analysis of resonant wireless power transfer. *IEEE Transactions on. Power Electronics*, 2014, 29(3): 1058-1063.

[30] Y H Chao, J Shieh, C T Pan, et al. A closed-form oriented compensator analysis for series-parallel loosely coupled inductive power transfer systems. *Proc. IEEE. PESC*, 2007: 1215-1220.

[31] G A J Elliott, S Raabe, G A Covic, et al. Multi-phase pick-ups for large lateral tolerance contactless power transfer systems. *IEEE Transactions on Industrial Electronics*, 2010, 57(5): 1590-1598.

[32] D L M G Egan, J Sullivan, G Hayes, et al. Power-factor-corrected single stage inductive charger for electric vehicle batteries. *IEEE Transactions on Industrial Electronics*, 2007, 54(2): 1217-1226.

[33] Z Pantic, S Lukic. Framework and topology for active tuning of parallel compensated receivers in wireless

power transfer systems. *IEEE Transactions on Power Electronics*, 2012, PP(99): 1-10.

[34] A C M D Queiroz. A generalized approach to the design of multiple resonance networks. *IEEE Transactions on Circuits and Systems I: Regular Papers*, 2006, 53(4): 918-927.

[35] A Casson, E Rodriguez Villegas. A review and modern approach to LC ladder synthesis. *Journal of Low Power Electronics and Applications*, 2011, 1(1): 20-44.

[36] G A Covic, J T Boys, A M W Tam, et al. Self-tuning pick-ups for inductive power transfer. *Proc. of IEEE Power Electronics Specialists Conference (PESC)*, 2008: 3489-3494.

[37] B Yang. Topology investigation of front end DC/DC converter for distributed power system. Ph.D. dissertation, Virginia Tech., Department of Electrical and Computer Engineering, Virginia, 2003.

[38] C Brun. Electrical and magnetical modelling of inductive coupled power transfer systems. Ph.D. thesis, École Polytechnique Fédérale De Lausanne, 2015.

[39] C S Wang, O H Stielau, G A Covic. Load models and their application in the design of loosely coupled inductive power transfer systems. *Proc. of IEEE Power System Conference*, 2000(2): 1053-1058.

[40] O H Stielau, G Covic. Design of loosely coupled inductive power transfer systems. *Proc. of IEEE Power System Technology Conference*, 2000(1): 85-90.

[41] Y Zhang, T Lu, Z Zhao, et al. Impact of source internal resistance on efficiency of four resonant wireless power transfer topologies. *Proc. of 17th IEEE Int. Conference on Electrical Machines and Systems (ICEMS)*, 2014: 1926-1930.

[42] N Bailian, C Y Chung, H L Chan. Design and comparison of parallel and series resonant topology in wireless power transfer. *Proc. of IEEE ICIEA*, 2013: 1832-1837.

[43] R J Calder, S H Lee, R D Lorenz. Efficient, MHz frequency, resonant converter for sub-meter (30 cm) distance wireless power transfer. *Proc. of IEEE Energy Conversion Congress and Exposition (ECCE)*, 2013: 1917-1924.

[44] B Lu, W Liu, Y Liang, et al. Optimal design methodology for LLC resonant converter. *Proc. of IEEE 21st Annual Applied Power Electronics Conference and Exposition*, 2006, 1(6): 19-23.

[45] H Leung, D McCormick, D Budgett, et al. Design methodology for inductive power transfer systems targeting high power implantable devices. *Proc. of IEEE International Symposium on Circuits and Systems (ISCAS)*, 2013: 2787-2791.

[46] I Nam, R Dougal, E Santi. Novel control approach to achieving efficient wireless battery charging for portable electronic devices. *Proc. of IEEE Energy Conversion Congress and Exposition (ECCE)*, 2012: 2482-2491.

[47] S Li, W Li, J Deng, et al. A double-sided LCC compensation network and its tuning method for wireless power transfer. *IEEE Transactions on Vehicular Technology*, 2015, 64(6): 2261-2273.

[48] Y Fu, H Bai. Design of a wireless charging system used in light-duty electrified automobiles. *Proc. of IEEE Transportation Electrification Conference and Expo. (ITEC)*, 2014: 1-6.

[49] Y Su, C Tang, S Wu, et al. Research of LCL resonant inverter in wireless power transfer system. *Proc. of IEEE Power Con.*, 2006: 1-6.

[50] C Zhu, C Yu, K Liu, et al. Research on the topology of wireless energy transfer device. *Proc. of IEEE VPPC*, 2008: 1-5.

[51] W Zhang, S Chung Won, C K Tse, et al. Load-independent duality of current and voltage outputs of a series- or parallel-compensated inductive power transfer converter with optimized efficiency. *IEEE Journal of Emerging and Selected Topics in Power Electronics,* 2015, 3(1): 137-146.

[52] J Sallan, J L Villa, A L lombart, et al. Optimal design of ICPT systems applied to electric vehicle battery charge. *IEEE Transactions on Industrial Electronics*, 2009, 56(6): 2140-2149.

[53] V Freschi, P Guglielmi. Wireless power transfer structure design for electric vehicle in charge while driving. *Proc. of IEEE Electrical Machines (ICEM)*, 2014: 2461-2467.

[54] C Y Huang, J T Boys, G A Covic. LCL pick-up circulating current controller for inductive power transfer systems. *IEEE Transactions on Power Electronics*, 2013, 28(4): 2081-2093.

[55] F Lu, H Hofmann, J Deng, et al. Output power and efficiency sensitivity to circuit parameter variations in double-sided LCC-compensated wireless power transfer system. *Proc. of IEEE Applied Power Electronics Conference and Exposition (APEC)*, 2015: 597-601.

[56] Q Zhu, L Wang, C Liao. Compensate capacitor optimization for kilowatt-level magnetically resonant wireless charging system. *IEEE Transactions on Industrial Electronics*, 2014, 61(12): 6758-6768.

[57] Z Pantic, S Bai, S M Lukic. ZCS LCC-compensated

resonant inverter for inductive-power-transfer application. *IEEE Transactions on Industrial Electronics*, 2011, 58(8): 3500-3510.

[58] M A Razzak, S Takamura, N Ohno, et al. Design of a novel T-LCL immittance conversion circuit for dynamic and non-linear loads. *Proc. of IEEE ICECE'06*, 2006: 13-16.

[59] C S Wang, G A Covic, O H Stielau. Investigating an LCL load resonant inverter for inductive power transfer applications. *IEEE Transactions on Power Electronics*, 2004, 19(4): 995-1002.

[60] S Dieckerhoff, M Ruan, R W De Doncker. Design of an IGBT-based LCL-resonant inverter for high-frequency induction heating. *Proc. of IEEE Thirty-Fourth IAS Annual Meeting Conference*, 1999(3): 2039-2045.

[61] N A Keeling, G A Covic, J T Boys. A unity-power-factor IPT pickup for high-power applications. *IEEE Transactions on Industrial Electronics*, 2010, 57(2): 744-751.

[62] M A Razzak, S Takamura, N Ohno, et al. Design of a novel T-LCL immittance conversion circuit for dynamic and non-linear loads. *Proc. of IEEE ICECE'06*, 2006: 13-16.

[63] T Latif, F N Rahman, M A Razzak, et al. Design & analysis of a sine wave inverter using forward converter and T-LCLC immittance conversion circuit. *Proc. of IEEE Applied Electrical Engineering and Computing Technologies (AEECT)*, 2013: 1-6.

[64] A K S Bhat. A generalized steady-state analysis of resonant converters using two-port model and Fourier-series approach. *IEEE Transactions on Power Electronics*, 1998, 13(1): 142-151.

[65] G L Fischer, H Doht. An inverter system for inductive tube welding utilizing resonance transformation. *Proc. of IEEE IAS Meeting*, 1994(2): 833-840.

[66] W Li, H Zhao, S Li, et al. Integrated compensation topology for wireless charger in electric and plug-in electric vehicles. *IEEE Transactions on Industrial Electronics*, 2015, 62(7): 4215-4225.

[67] H Chang-Yu, J T Boys, G A Covic, et al. LCL pick-up circulating current controller for inductive power transfer systems. *IEEE Energy Conversion Congress and Exposition (ECCE)*, 2010: 640-646.

[68] K Lee, Z Pantic, S Lukic. Field containment in dynamic wireless charging systems through source-receiver interaction. *IEEE Energy Conversion Congress and Exposition (ECCE)*, 2013: 3658-3663.

[69] A Triviño, D Fernandez, J A Aguado, et al. Sensitivity analysis of component's tolerance in inductively coupled power transfer system. *Proc. of IEEE IEVC*，2014: 1-6.

[70] H L Li, A P Hu, G A Covic, et al. A new primary power regulation method for contactless power transfer. *Proc. of IEEE Conference on Industrial Technology*, 2009: 1-5.

[71] H H Wu, G A Covic, J T Boys, et al. A series tuned inductive power transfer pickup with a controllable AC voltage output. *IEEE Transactions on Power Electronics*, 2011, 26(1): 98-109.

[72] H H Wu, J T Boys, G A Covic. An AC processing pickup for IPT systems. *IEEE Transactions. on Power Electronics*, 2010, 25(5): 1275-1284.

[73] Y H Chao, J J Shieh, C T Pan, et al. A primary-side control strategy for series-parallel loosely coupled inductive power transfer systems. *Proc. IEEE Conf. Ind. Electron. Appl.*, 2007: 2322-2327.

[74] P Si, A P Hu, J W Hsu, et al. Wireless power supply for implantable biomedical device based on primary input voltage regulation. *Proc. IEEE Conf. Ind. Electron. Appl.* 2007: 235-239.

[75] U K Madawala, M Neath, D J Thrimawithana. A power-frequency controller for bidirectional inductive power transfer systems. *IEEE Transactions on Industrial Electronics*, 2013, 60(1): 310-317.

[76] X Qu, W Zhang, S C Wong, et al. Design of a current-source-output inductive power transfer led lighting system. *IEEE Journal of Emerging Sel. Topics Power Electronics*, 2015, 3(1): 306-314.

[77] M Yilmaz, P T Krein. Review of battery charger topologies, charging power levels, and infrastructure for plug-in electric and hybrid vehicles. *IEEE Transactions on Power Electronics*, 2013, 28(5): 2151-2169.

[78] W Zhang, S C Wong, Q Chen. Design for efficiency optimization and voltage controllability of series-series compensated inductive 745 power transfer systems. *IEEE Transactions on Power Electronics*, 2014, 29(1): 191-200.

[79] J Hou, Q Chen, X Ren, et al. Precise characteristics analysis of series/series-parallel compensated contactless resonant converter. *IEEE Journal of Emerging and Selected Topics in Power Electronics*, 2015, 3(1): 101-110.

[80] H L Li, A P Hu, G A Covic. A direct AC-AC converter for inductive power-transfer systems. *IEEE Transactions on Power Electronics*, 2012, 27(2): 661-668.

[81] A W Green, J T Boys. 10 kHz inductively coupled power transfer-concept and control. *Proc. of IEEE International Conference on Power Electronics and Variable Speed*

Drives, 1994: 694-699.

[82] H H Wu, A Gilchrist, K Sealy, et al. A high efficiency 5kW inductive charger for EVs using dual side control. *IEEE Transactions on Industrial Informatics*, 2012, 8(3): 585-595.

[83] H H Wu, A Gilchrist, K Sealy, et al. Design of symmetric voltage cancellation control for LCL converters in inductive power transfer systems. *Proc. of IEEE Electric Machines & Drives Conference (IEMDC)*, 2011: 866-871.

[84] M Kesler. Highly resonant wireless power transfer: safe, efficient, and over distance. *Technical Note*, WiTricity Corporation, 2013.

[85] C Fernandez, O Garcia, R Prieto, et al. Overview of different alternatives for the contact-less transmission of energy. *Proc. of. IEEE IECON*, 2002(2): 1318-1323.

[86] J M Miller, A Daga. Elements of Wireless power transfer essential to high power charging of heavy duty vehicles. *IEEE Transactions on Transportation Electrification*, 2015, 1(1): 26-39.

[87] K Aditya, S Williamson. Advanced controller design for a series-series compensated inductive power transfer charging infrastructure using asymmetrical clamped mode control. *Proc. of IEEE Applied Power Electronics Conference and Exposition (APEC)*, 2015: 2718-2724.

[88] J M Burdío, L A Barragan, L A Monterde, et al. Asymmetrical voltage-cancellation control for full-bridge series resonant inverters. *IEEE Transactions. on Power Electronics*, 2004, 19(2): 461-469.

[89] http://www.sae.org/servlets/pressRoom?OBJECT_TYPE=PressReleases&PAGE=showRelease&RELEASE_ID=2296. Accessed online on 11.09.2015.

[90] K N Mude, M Bertoluzzo, G Buja. Inductive characteristics of different coupling setups for wireless charging of an electric city-car. *Proc. of IEEE IEVC 2014*, 2014: 1-6.

[91] V Prasanth. Wireless power transfer for E-mobility. Master of science thesis, Delft University of Technology, Faculty of Electrical Engineering, Mathematics and Computer Science, Electrical Power Processing, 2012.

Appendix

The design guidelines of primary and secondary two-element resonant topologies is explained in following steps.

1 Finding the load resistance

From Ref. [8], it can be observed that reflected resistance (R_{O}) decreases during the charging process at constant current, getting a minimum when the battery voltage reaches the maximum voltage, and then increases again, in a somewhat appreciable manner, during the charging process at constant voltage. From R_{O}, the resistance reflected at the input of diode rectifier, i.e. the equivalent load resistance R_{L} for the WPTS, is determined as

$$R_{\mathrm{L}}=\frac{8}{\pi^2}R_{\mathrm{O}}=\frac{8}{\pi^2}\frac{V_{DC}^2}{P_{\mathrm{B}}} \tag{A1}$$

2 Load current estimation

From Ref. [11] and formula (6), expression of the load current, that is equal to the current in the receiving coil, is obtained from formula (2). It is

$$I_{\mathrm{L}}=\sqrt{\frac{P_{\mathrm{L}}}{R_{\mathrm{L}}}}=\frac{P_{\mathrm{B}}}{\frac{2\sqrt{2}}{\pi^2}V_{\mathrm{R}}} \tag{A2}$$

But formula (12) can be rewritten as considering the formula (8)～(10)

$$I_{\mathrm{L}}=\frac{\overline{V}_{\mathrm{s}}}{\mathrm{j}\omega M}\eta_i \tag{A3}$$

From (A2), the mutual inductance can be evaluated taking into account an estimated efficiency of 0.95.

3 Mutual inductance and coupling coefficient calculation

$$M=I_{\mathrm{L}}\frac{\omega}{\overline{V}_{\mathrm{s}}\eta_i} \tag{A4}$$

Given the equivalent R_{L} and the working frequency, the specification for Q_{R} can be easily translated into specification for L_{R} by means of formula (11) and the coupling coefficient is given by

$$k=\frac{\eta_{\mathrm{maz}}}{(1-\eta_{\mathrm{maz}})Q_{\mathrm{T}}Q_{\mathrm{R}}} \tag{A5}$$

4 Calculation of self-inductances

Self-inductances L_T and L_R can be evaluated as

$$L_{\mathrm{T}}=\frac{P_{\mathrm{L}}}{\omega Q_{\mathrm{R}}k^2|\overline{I}_{\mathrm{s}}|^2} \tag{A6}$$

$$L_{\mathrm{R}}=\frac{\lfloor V_{\mathrm{R}}^2\rfloor}{(\omega Q_{\mathrm{R}})^2k^2L_{\mathrm{T}}|\overline{I}_{\mathrm{s}}|^2} \tag{A7}$$

The compensation capacitance (C_{T} and C_{R}) values can be obtained for different topologies by knowing values of L_{T}, L_{R} and ω.

K. N. Mude received his B.Tech. degree in Electrical Engineering from Sri Venkateshwara University, Tirupati, India, in 2008, and his M.Tech. degree in Electrical Engineering from the Motilal Nehru National Institute of Technology, Allahabad, India, in 2010. From 2010 to 2011, he was a Lecturer at Amity University, Noida, India. He graduated his Ph.D degree in Electrical Engineering from University of Padova, Italy, in March 2015. Presently he is working as senior electrical researcher with solace power, Canada. Prior to this he was working with Systec R&D, Porto, Portugal and he also served as an Asst. Professor in Amrita Vishwa Vidyapeetham University, Bengaluru campus, India. He received Prestigious European fellowship CARIPARO sponsored by Italian Bank, for three years of his doctoral study. He was invited for talk on Wireless Battery chargers in various organizations in India and abroad. His current area of research includes, Wireless Power Transfer, Battery chargers. He organized and chaired special sessions in the area of Wireless Power Transfer.

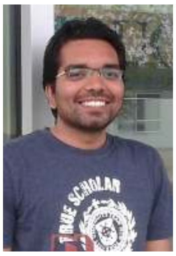

K. Aditya (S’14-M’17) received the B.E. degree from Bharati Vidyapeeth University, Pune, India; the M.Tech. degree from Indian Institute of Technology (Banaras Hindu University), Varanasi, India; and the Ph.D. degree from the University of Ontario Institute of Technology (UOIT), Oshawa, ON, Canada, in 2009, 2012, and 2016, respectively, all in electrical engineering. He was awarded the IIT (BHU) Gold Medal, for securing highest academic standing among all the electrical engineering students of 2012 cohort.

From July 2017 to Nov 2017, he worked as a Research Fellow for Rolls-Royce@NTU Corporate Lab at Nanyang Technological University, in Singapore. Since Dec 2017, he is working as a Hardware Engineer with BorgWarner waterloo Inc., Kitchener, ON, Canada. His research interests include power electronics and control applied to Wireless Charging, electrical energy storage system and transportation electrification. He is a Member of the IEEE.